

UNCLASSIFIED  
**CONFIDENTIAL**Copy 4  
RM L58C11

C 2

**NACA**

# RESEARCH MEMORANDUM

WIND-TUNNEL INVESTIGATION AT A MACH NUMBER OF 2.01 OF  
FOREBODY STRAKES FOR IMPROVING DIRECTIONAL STABILITY  
OF SUPERSONIC AIRCRAFT

By Cornelius Driver

Langley Aeronautical Laboratory  
Langley Field, Va.

**LIBRARY COPY**

MAY 20 1958

LANGLEY AERONAUTICAL LABORATORY  
LIBRARY, NACA  
LANGLEY FIELD, VIRGINIA

CLASSIFIED DOCUMENT

This material contains information affecting the National Defense of the United States within the meaning of the espionage laws, Title 18, U.S.C., Secs. 793 and 794, the transmission or revelation of which in any manner to an unauthorized person is prohibited by law.

**NATIONAL ADVISORY COMMITTEE  
FOR AERONAUTICS**

WASHINGTON

May 26, 1958

**CONFIDENTIAL**

UNCLASSIFIED

CLASSIFICATION CHANGED  
TO UNCLASSIFIED  
DATE 10-28-66  
BY JPH #33  
FRC

CONFIDENTIAL

UNCLASSIFIED

## NATIONAL ADVISORY COMMITTEE FOR AERONAUTICS

## RESEARCH MEMORANDUM

WIND-TUNNEL INVESTIGATION AT A MACH NUMBER OF 2.01 OF  
FOREBODY STRAKES FOR IMPROVING DIRECTIONAL STABILITY

## OF SUPERSONIC AIRCRAFT

By Cornelius Driver

## SUMMARY

An investigation has been conducted in the Langley 4- by 4-foot supersonic pressure tunnel to determine the effects of forebody strakes on the aerodynamic characteristics in sideslip of a delta-wing airplane model at a Mach number of 2.01. The model was tested with two different vertical-tail locations; one configuration had a single vertical tail mounted at the center line of the body, and the second configuration had twin tails mounted on the wing at the 0.50-semispan station. A body-alone configuration was also tested with strakes of varying thickness and vertical location.

The presence of the strakes increased the directional-stability level for both vertical-tail arrangements. The increase was caused, in part, by favorable effects on the forebody and, in part, by favorable flow changes at the vertical tail. Strake locations below the horizontal center line of the body did not result in significant improvements in the directional-stability level. Although tests of individual windward and leeward strakes indicated that thickness affected the contribution of the windward strake, there was little significant improvement due to thickness when both strakes were present.

Results of pressure tests for a forebody show that the presence of the strakes provides a stabilizing influence on the forebody which is consistent with the results of force tests.

## INTRODUCTION

One of the problems frequently encountered with supersonic aircraft is that of the low-directional-stability level that occurs with increasing

CONFIDENTIAL

UNCLASSIFIED

Mach number and increasing angle of attack. This problem stems from two main sources; one source is the highly unstable wing-body combinations that result from the use of high-fineness-ratio bodies and far rearward centers of gravity, and the other source is the decrease in vertical-tail effectiveness that results from a decrease in tail lift-curve slope with increasing Mach number and from the effects of forebody and wing vorticity with increasing angle of attack.

A logical way to attack the problem of low directional stability would be to seek means whereby the level of instability of the wing-body combination might be reduced. In this way the tail size and load might be reduced. Another course to pursue would be to seek means of increasing the tail effectiveness other than by merely increasing the size of the vertical tail.

Recent tests at subsonic speeds have indicated that significant improvement in the stability level for wing-body combinations might be obtained at high angles of attack through the use of forebody fins or strakes. These strakes act in such a way as to provide a directionally stabilizing moment increment over the forebody and have been found to be useful as an aid to spin recovery (refs. 1 and 2) and as a means of increasing directional stability at high angles of attack (ref. 3). The strakes might also be expected to affect the forebody vorticity and thereby have an effect on the tail contribution.

In order to determine if the use of strakes might be advantageous at supersonic speeds, an investigation has been conducted at a Mach number of 2.01 in the Langley 4- by 4-foot supersonic pressure tunnel of various strake arrangements. The model used in the investigation was a tailless configuration and had a  $60^\circ$  delta wing. Tests were made with both a single body-mounted vertical tail and twin wing-mounted tails in order to determine the effects of strakes on vertical-tail effectiveness.

The investigation included the effects of strake length and radial position, the relative effects of windward and leeward strakes, and the effects of strake thickness and vertical location on two cylindrical body configurations. Subsequent to the completion of the force tests a forebody pressure model was tested to provide an insight into the changes in pressure on the forebody caused by the presence of the strakes. The results of force tests and an example of the results of pressure tests are presented.

## SYMBOLS

The results are presented as force and moment coefficients with lift, drag, and pitching moment referred to the stability axis system and rolling moment, yawing moment, and side force referred to the body axis system (fig. 1). The reference center of moments was at a station on the body center line which corresponds to a location at 7.75 percent of the wing mean geometric chord.

$C_L$	lift coefficient, $F_L/qS$
$C_D'$	approximate drag coefficient $F_D'/qS$ equal to true drag coefficient at $\beta = 0^\circ$
$C_m$	pitching-moment coefficient, $M_{Y_S}/qS\bar{c}$
$C_l$	rolling-moment coefficient, $M_X/qSb$
$C_n$	yawing-moment coefficient, $M_Z/qSb$
$C_Y$	side-force coefficient, $F_Y/qS$
$F_L$	lift force
$F_D'$	approximate drag (true drag at $\beta = 0^\circ$ )
$M_Y$	moment about Y-axis
$M_X$	moment about X-axis
$M_Z$	moment about Z-axis
$F_Y$	side force
$q$	free-stream dynamic pressure
$S$	wing area including fuselage intercept
$b$	wing span
$\bar{c}$	wing mean geometric chord (MGC)

M	free-stream Mach number
$\alpha$	angle of attack of fuselage reference line, deg
$\beta$	angle of sideslip of fuselage reference line, deg
$C_{n\beta}$	directional-stability parameter, $\partial C_n / \partial \beta$
$C_{l\beta}$	effective-dihedral parameter, $\partial C_l / \partial \beta$
$C_{Y\beta}$	side-force parameter, $\partial C_Y / \partial \beta$
Subscript:	
s	denotes stability axis system
Configurations:	
B <sub>1</sub>	body shown in figures 2(a) and 3; body coordinates given in table I
B <sub>2</sub>	body shown in figure 4(a); body coordinates given in table I
W <sub>1</sub>	60° delta wing shown in figure 2(b)
S <sub>1</sub> , S <sub>2</sub> , . . . S <sub>8</sub>	strake configurations shown in figures 3 and 4
V <sub>1</sub>	single tail mounted on fuselage, figure 2
V <sub>2</sub>	two tails mounted at 0.50b/2 on upper surface of wing as shown in figure 2

#### MODELS AND APPARATUS

Two different models were used in the force tests. The first model was a body-alone configuration and the second model was a wing-body-tail configuration. The body coordinates of the models are given in table I and the geometric characteristics are given in table II. Details of the strakes are presented in figures 3 and 4.

Eight different strake arrangements were tested. For the  $S_1$  configuration (fig. 3) the strakes had exposed semispans of 0.25 inch, were mounted on the body center line, were 0.0625 inch thick, and extended rearward 37.7 percent of the body length. The  $S_2$  configuration was obtained by moving the  $S_1$  configuration radially to a  $45^\circ$  position (fig. 3). The  $S_3$  configuration had the same span and thickness as  $S_1$  configuration but extended rearward to the leading edge of the wing (47.1 percent of the body length). The model was tested with strakes on and off and with the vertical tail on and off. Details of the vertical tails and the wing are shown in figure 2(b).

For the  $S_4$  and  $S_5$  configurations (fig. 4(a)) the strakes had semispans 0.1 of the maximum model diameter, were mounted on the body center line ( $B_2$ ), were 0.25 and 0.125 inch thick, respectively, and extended rearward 30 percent of the body length. Both of these configurations ( $S_4$  and  $S_5$ ) were also tested with only a single strake installed. Lee-ward and windward effects were determined by rolling the model  $180^\circ$ . The  $S_6$  configuration was a single-strake configuration identical in span and length to configuration  $S_1$  but with the strake beveled to a sharp edge (fig. 4(b)).

The  $S_7$  configuration had the same thickness and semispan as the  $S_1$  configuration but was mounted  $1/2$  inch below the center line of the body (fig. 4(b)). The  $S_8$  configuration was obtained by attaching an 0.032-inch-thick plate to the bottom of the  $S_7$  configuration to obtain the same plan-form area as configurations  $S_4$  and  $S_5$ .

Subsequent to the completion of the force tests, a forebody pressure model was tested which had the same body coordinates as the forebody for the wing-body-tail configuration ( $B_1$ ). Details of the pressure model are shown in figure 3.

Force measurements were made through the use of a six-component internal strain-gage balance. The model was mounted in the tunnel on a remote-controlled rotary sting. The sting-angle range was varied from  $0^\circ$  to about  $25^\circ$  at various roll angles from  $0^\circ$  to  $90^\circ$ .

## TESTS, CORRECTIONS, AND ACCURACY

The test conditions are summarized as follows:

M . . . . .	2.01
Stagnation temperature, $^{\circ}\text{F}$ . . . . .	100
Stagnation pressure, lb/sq in. abs . . . . .	1440
Reynolds number based on $\bar{c}$ . . . . .	$2.68 \times 10^6$

The stagnation dewpoint was maintained sufficiently low ( $-25^{\circ}\text{F}$  or less) that no condensation effects were encountered in the test section.

The angles of attack and sideslip were corrected for the deflection of the balance and sting under load. The Mach number variation in the test section was approximately  $\pm 0.01$ , and the flow-angle variation in the vertical and horizontal planes did not exceed about  $\pm 0.1^{\circ}$ . No corrections to the data were considered necessary to account for these flow variations. The base pressure was measured, and the drag was adjusted to a base pressure equal to free-stream static pressure.

The estimated repeatability of the individual measured quantities is as follows:

$C_L$ . . . . .	$\pm 0.0003$
$C_D$ . . . . .	$\pm 0.0010$
$C_m$ . . . . .	$\pm 0.0004$
$C_z$ . . . . .	$\pm 0.0004$
$C_n$ . . . . .	$\pm 0.0001$
$C_y$ . . . . .	$\pm 0.0015$
$\alpha$ , deg . . . . .	$\pm 0.2$
$\beta$ , deg . . . . .	$\pm 0.2$

## DISCUSSION

### Complete Configuration

An example of the variation of the lateral characteristics with sideslip is presented in figure 5 to indicate the linearity of the test data. The subsequent sideslip derivatives presented (figs. 6 to 9) were obtained from increments measured in tests run at  $0^{\circ}$  and  $4^{\circ}$  sideslip through the angle-of-attack range.

Single vertical tail.- For the model with the single vertical tail (fig. 6), the presence of the strakes postponed the characteristic decrease in directional stability with angle of attack; therefore, the angle of attack at which directional instability occurred was increased from  $12.5^{\circ}$  to  $20^{\circ}$ . The results for the vertical tail off (fig. 6) show that the addition of the strakes provides a stabilizing  $C_{n\beta}$  increment with a positive increment in  $C_{Y\beta}$ , and thus a decrease in the destabilizing side force ahead of the center of moments is indicated. For the vertical tail on, however, the stabilizing  $C_{n\beta}$  increment provided by the strakes is about twice that for the tail-off condition with an increase in the side force provided by the vertical tail. Since the tail-off  $C_{Y\beta}$  effects on the forebody are still present, the additional stabilizing increment provided by the strakes with the tail on probably result from favorable flow changes at the vertical tail. At subsonic speeds the presence of the strakes for a somewhat different configuration (ref. 3) provided similar forebody improvements; however, the tail contribution at subsonic speeds was decreased in the presence of the strakes.

The strakes provide a large negative  $C_{l\beta}$  increment for the wing-body configuration, and this increment indicates a large effect on the lift of the leeward wing panel (fig. 6). The strake effects on  $C_{l\beta}$ , for the vertical tail on, are consistent with the results for  $C_{n\beta}$  and  $C_{Y\beta}$  since a stabilizing flow change at the vertical tail would also result in a larger negative  $C_{l\beta}$  increment due to the vertical tail.

Twin vertical tails.- For the configuration with the twin tails at the 0.50b/2 station (fig. 7) the stabilizing increment in  $C_{n\beta}$  provided by the strakes is somewhat larger than for the single-tail configuration, with about the same changes in  $C_{Y\beta}$  as for the single-tail configuration. Even though the twin tails have twice the lateral area of the single-tail configuration and provide large increases in  $C_{Y\beta}$ , they provide about the same  $C_{l\beta}$  increment.

Effect of strake radial position.- For one configuration ( $S_2$ , fig. 3) the strakes were moved radially on the forebody from the horizontal center-line position to a position  $45^{\circ}$  below the horizontal center line to determine the effects of strake radial location. The results are shown in figure 8 and indicate that for models with both the single



and twin tails the presence of the strakes in the  $45^\circ$  plane below the horizontal center line provided lower levels of directional stability than the strake-off case. This may result because the strakes in the  $45^\circ$  location add lateral area ahead of the center of moments. In addition, a less negative  $C_{l_\beta}$  results with the  $45^\circ$  strakes than for the strakes mounted on the center line.

Effect of strake length.- For another configuration ( $S_3$ , fig. 3), the strakes were extended on the horizontal center line to the wing leading edge. These results are presented in figure 9 and show about the same improvements in directional stability as did the shorter strakes.

Longitudinal characteristics.- The effects of the presence of strakes and of the strake length on the longitudinal characteristics are presented in figure 10. The presence of the strakes had little effect on the static margin, lift-curve slope, or drag due to lift. The main result appears to be an increase in the nonlinearity of the pitching-moment curve with an increased tendency toward pitchup. The effects of increasing the strake length to the leading edge of the wing were small but tended to further decrease the static margin and to increase the tendency toward pitchup at the higher angles of attack (fig. 10).

#### Body-Alone Configuration

Basic results.- In order to determine more fully the effects of strakes, tests were made of a body-alone configuration having a single windward or leeward strake installed. Results for the single-strake configurations are presented in figures 11 and 12.

The addition of the 1/4-inch-thick strakes to the body alone ( $S_4$ , fig. 4(a)) caused a sizeable increase in the directional-stability level above angles of attack of  $12^\circ$  (fig. 11). The results for  $C_{Y_\beta}$  indicate a positive increment in  $C_{Y_\beta}$  which is consistent with the increase in directional stability. No significant changes were indicated in the results for  $C_{l_\beta}$ .

Tests of the 1/4-inch-thick single-strake configurations (both windward and leeward) indicate that the effectiveness of the windward strake appears to increase with increasing angle of attack, but the increase in effectiveness is not realized when both strakes are present (fig. 11). The presence of mutual interference effects is indicated since the increments provided by each single strake (fig. 11) add up to more than the total stability level provided by both strakes. Tests

with the 1/8-inch-thick strakes (fig. 12) show about the same improvement in the directional-stability level as do the 1/4-inch-thick strakes (fig. 11).

Effects of thickness.- The effects of strake thickness shown in figure 13 are relatively small and indicate that the thinner strakes provided slightly higher levels of directional stability. Subsequent to the tests of the 1/8-inch-thick strake, the single 1/4-inch strake was beveled to a sharp edge ( $S_6$ , fig. 4(b)) and tested in the windward position only. A comparison of thickness effects on the windward strake only is shown in the lower part of figure 13 which indicates that the beveled strake caused about the same increase in  $C_{n\beta}$  with angle of attack as the 1/8-inch strake but caused no significant increase in the maximum directional-stability level.

Effect of vertical location.- In an effort to find the effects of vertical location, the strakes were installed 1/2 inch below the horizontal center line, both with the same exposed span of 0.1-inch body diameter ( $S_7$ , fig. 4(b)) and with a plate attached to the bottom of the low strake to increase the plan-form area in the low position to the same value as when the strakes were located on the center line of the body ( $S_8$ ). Although the low strakes did not offer any improvement in the directional-stability level at low values of  $\alpha$ , the low strake with the plate attached did show some improvement above angles of attack of  $16^\circ$  (fig. 14).

### Pressure Measurements

Subsequent to the completion of the force tests a forebody pressure model was tested to provide an insight into the changes in pressure on the forebody caused by the presence of the strakes.

Representative results obtained at  $\alpha = 16^\circ$  and  $\beta = 4^\circ$  are presented in figure 15 where only the side-force component of the radial pressure distributions is shown. The positive values of  $C_y$  represent stabilizing side forces, whereas the negative values of  $C_y$  represent destabilizing side forces.

These results indicate that the presence of the strakes causes a more negative pressure field above the strakes, with the largest increase on the windward side of the forebody. The primary effect of the increased negative pressure field on the windward side is an increase in the stabilizing side force above the strake (fig. 15). This effect may be explained by the expansion which occurs above the windward strake as it becomes more inclined to the relative wind with increasing sideslip.

Conversely, the presence of the strakes causes a large increase in the positive pressure field below the strakes. The primary effect of the positive pressure field is on the leeward side where destabilizing side forces below the strake position are changed to stabilizing side forces. This effect results as the leeward strake becomes increasingly normal to the relative wind with increasing sideslip, and a damming of the flow occurs with a corresponding increase in pressure below the strake. These changes in loading on the forebody, indicated by the pressure tests, are consistent with wing-body and wing-body-strake force-test results (figs. 6 and 7). Vertical-tail pressure measurements and flow-angle measurements at the vertical tail would be necessary to account for that portion of the directional-stability improvement attributed to flow changes at the vertical tail.

### CONCLUSIONS

An investigation has been conducted in the Langley 4- by 4-foot supersonic pressure tunnel at a Mach number of 2.01 to determine the effects of forebody strakes on the aerodynamic characteristics in sideslip of a tailless delta-wing airplane model. The model was tested with two different vertical-tail locations; one configuration had the vertical tail on the center line of the body and the other had twin tails on the wing at the 0.50-semispan position. The results of the investigation indicate the following conclusions:

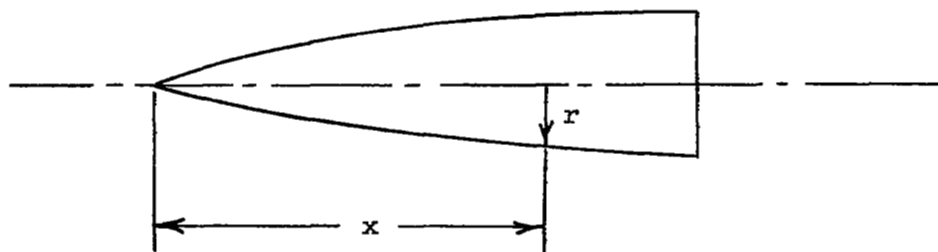
1. The presence of strakes increases the directional-stability level for both vertical-tail arrangements. The increase is caused, in part, by favorable effects on the forebody and, in part, by favorable flow changes at the vertical tail.
2. Strakes mounted below the maximum body diameter provide no significant improvements in the directional-stability level.
3. Although tests of single strakes indicate that thickness affects the contribution of the windward strake, there is little significant improvement in directional stability due to thickness when both strakes are present.
4. Initial pressure-test results of a forebody, which are consistent with the results of the force tests, show that the presence of the strakes provides a stabilizing influence on the forebody.

Langley Aeronautical Laboratory,  
National Advisory Committee for Aeronautics,  
Langley Field, Va., February 24, 1958.

## REFERENCES

1. Klinar, Walter J.: A Study by Means of a Dynamic-Model Investigation of the Use of Canard Surfaces As an Aid in Recovering From Spins and As a Means for Preventing Directional Divergence Near the Stall. NACA RM L56B23, 1956.
2. Paulson, John W., and Boisseau, Peter C.: Low-Speed Investigation of the Effect of Small Canard Surfaces on the Directional Stability of a Sweptback-Wing Fighter-Airplane Model. NACA RM L56F19a, 1956.
3. Sleeman, William C., Jr.: Investigation at High Subsonic Speeds of the Effects of Various Horizontal Fuselage Forebody Fins on the Directional and Longitudinal Stability of a Complete Model Having a  $45^\circ$  Sweptback Wing. NACA RM L56J25, 1957.

TABLE I. - BODY COORDINATES



Body 1

x, in.	r, in.
0	0
.297	.076
.627	.156
.956	.233
1.285	.307
1.615	.378
1.945	.445
2.275	.509
2.605	.573
2.936	.627
3.267	.682
3.598	.732
3.929	.780
4.260	.824
4.592	.865
4.923	.903
5.255	.940
5.587	.968
5.920	.996
6.252	1.020
6.583	1.042
18.648	1.75
37.000	1.75

} Conical section

Body 2

x, in.	r, in.
0	0
.30	.300
6.00	.963
7.00	1.073
8.00	1.176
9.00	1.262
10.00	1.335
11.00	1.394
12.00	1.441
13.00	1.474
14.00	1.493
15.00 to 30.00	1.500

TABLE II.- GEOMETRIC CHARACTERISTICS

## Body:

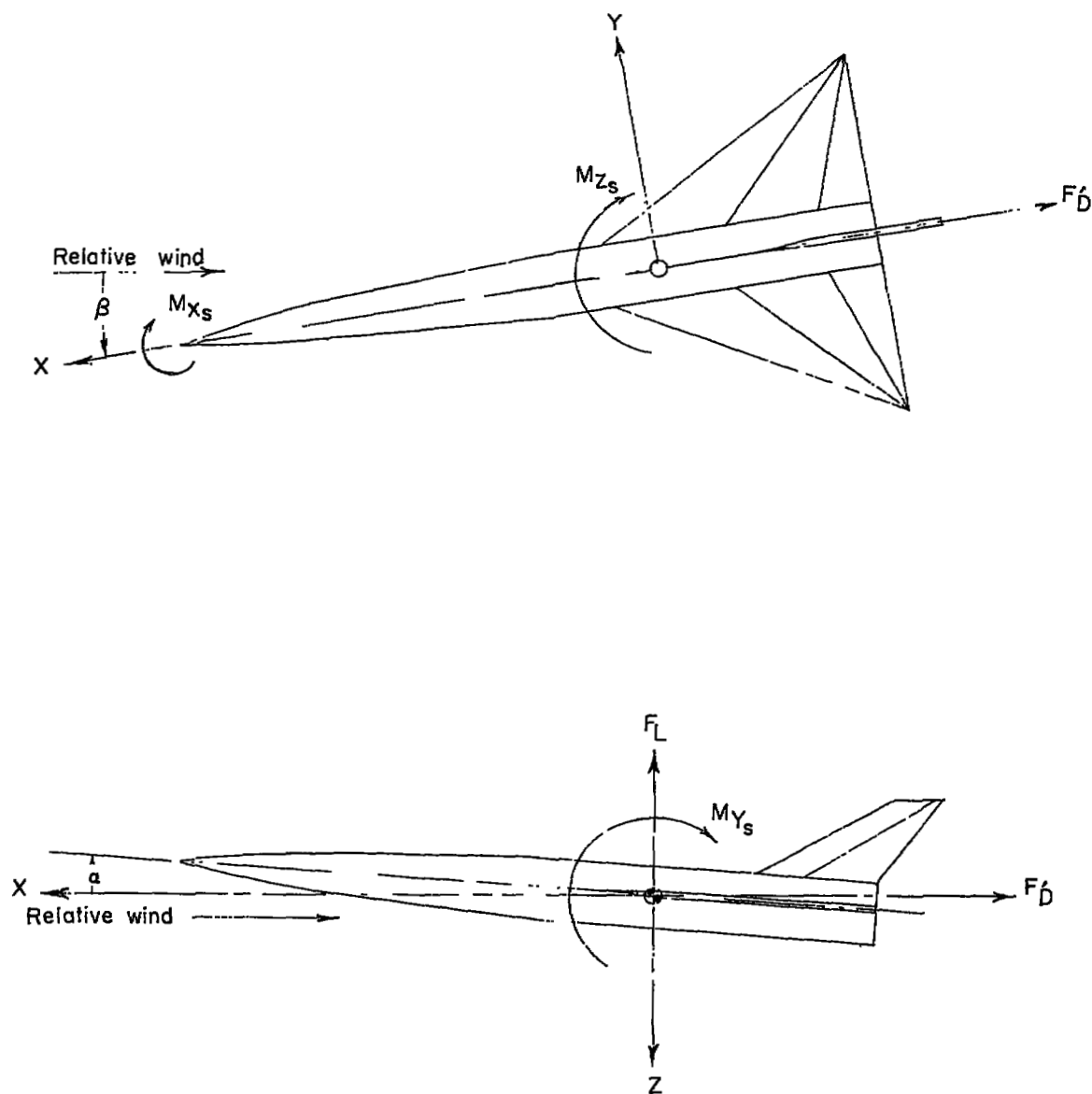
Maximum diameter, in. . . . .	3.50
Length, in. . . . .	37.00
Base area, sq in. . . . .	9.621
Fineness ratio . . . . .	10.57

## Delta Wing:

Total span, in. . . . .	22.56
Chord at body-wing intersection, in. . . . .	16.51
Mean geometric chord, in. . . . .	13.027
Total area, sq ft . . . . .	1.53
Aspect ratio . . . . .	2.31
Thickness ratio . . . . .	0.036
Leading-edge half-angle, normal to leading edge, deg . . .	5
Trailing-edge half-angle, normal to trailing edge, deg . .	5
Sweep . . . . .	60
Section . . . . .	Hexagonal

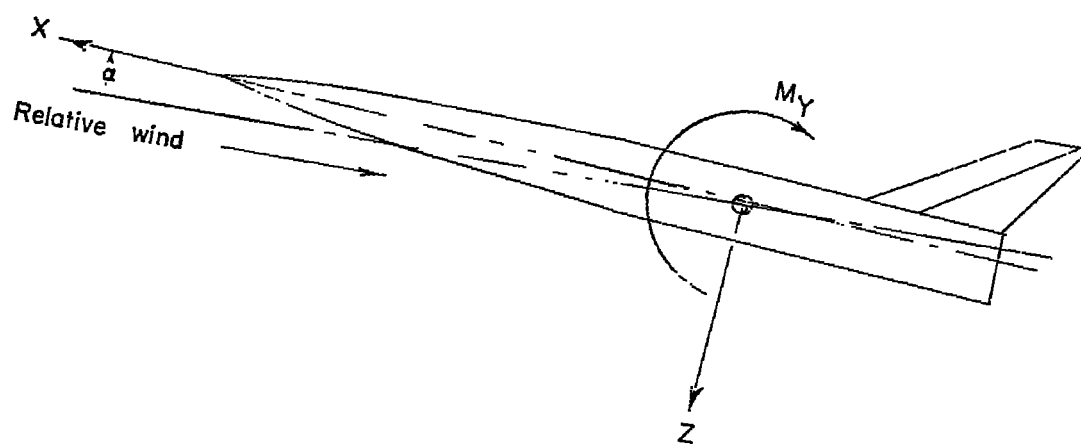
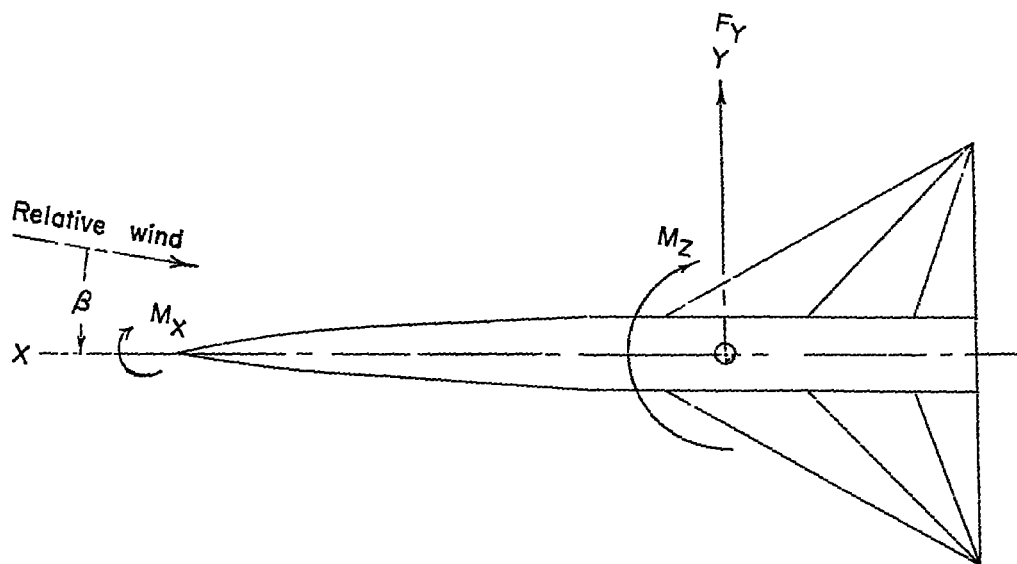
## Vertical Tail:

Area exposed, sq ft . . . . .	0.163
Span exposed, in. . . . .	5.10
Aspect ratio (panel) . . . . .	1.11
Sweep of leading edge, deg . . . . .	60
Section . . . . .	0.188 slab
Leading-edge half-angle, normal to leading edge, deg . . .	5
Root chord . . . . .	7.00
Tip chord . . . . .	2.20



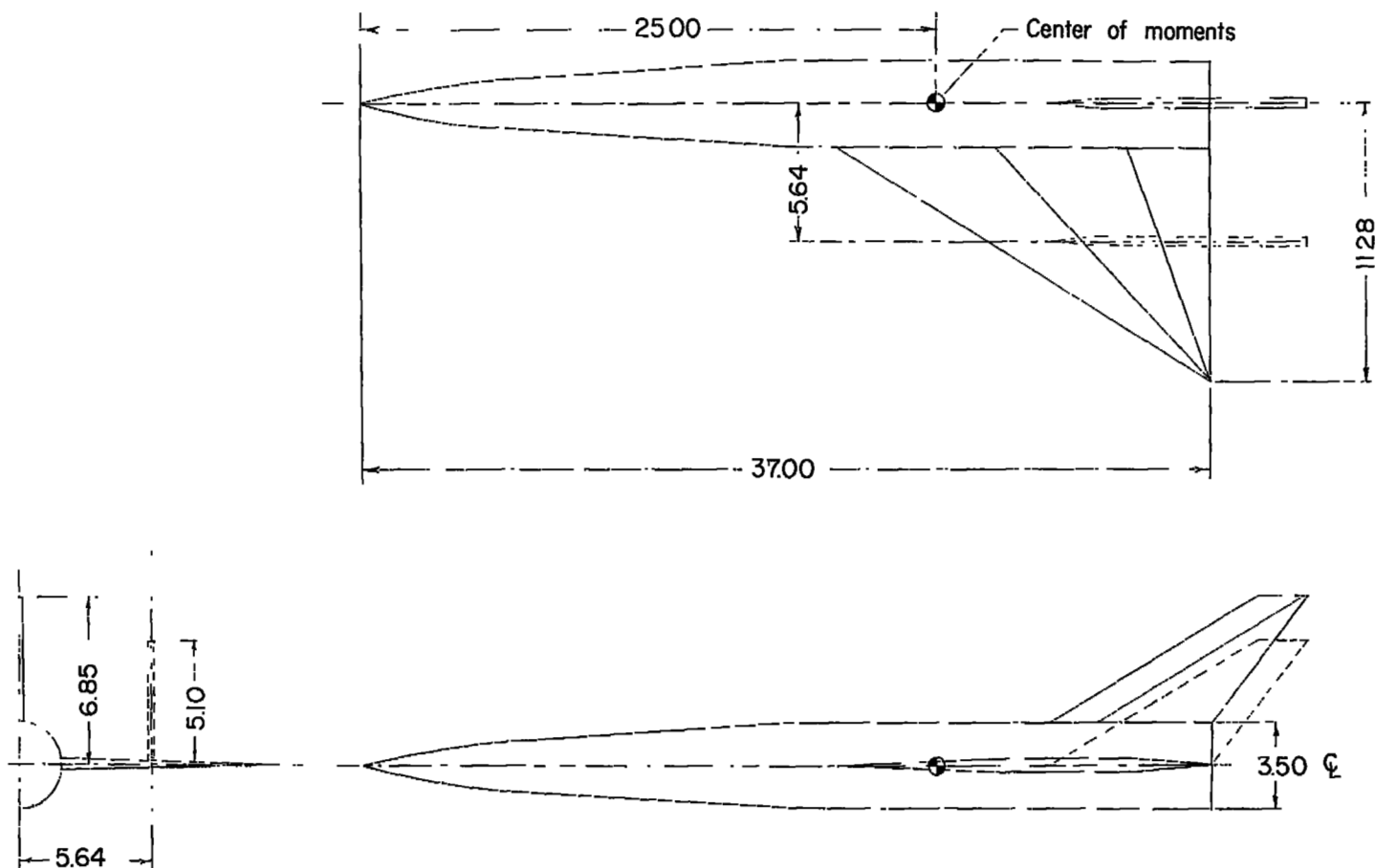
(a) Stability axis.

Figure 1.- Axes systems. Arrows indicate positive directions.



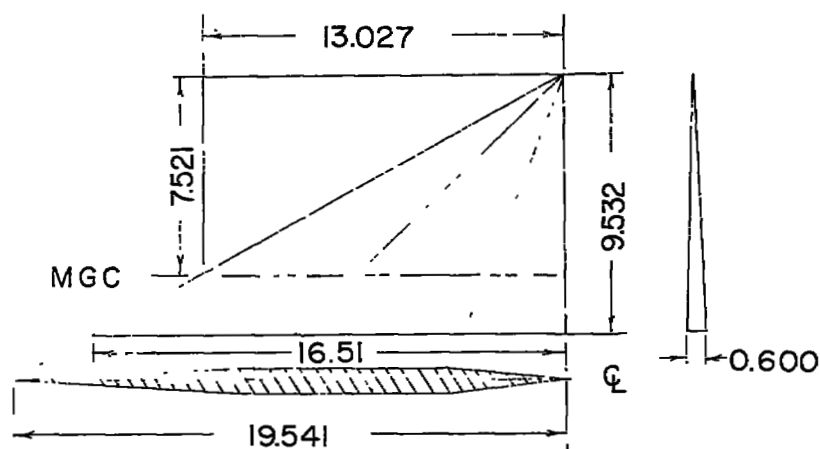
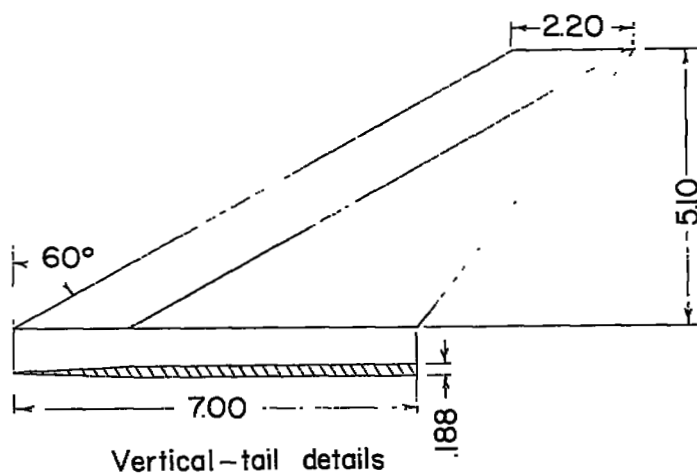
(b) Body axis.  
Figure 1.- Concluded.





(a) Complete model with body 1.

Figure 2.- Details of model.



Wing details

(b) Details of wing and vertical tail.

Figure 2.- Concluded.

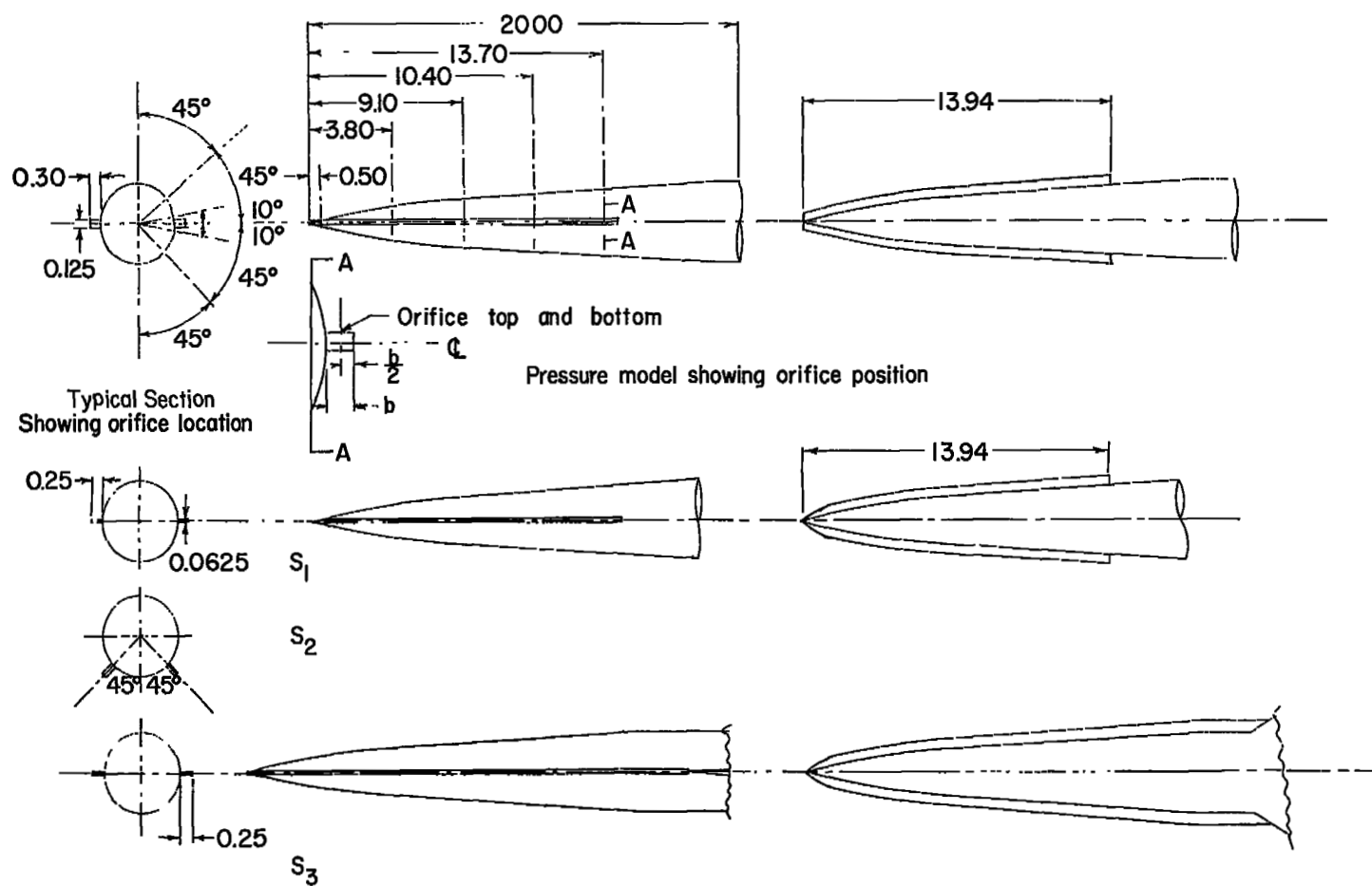
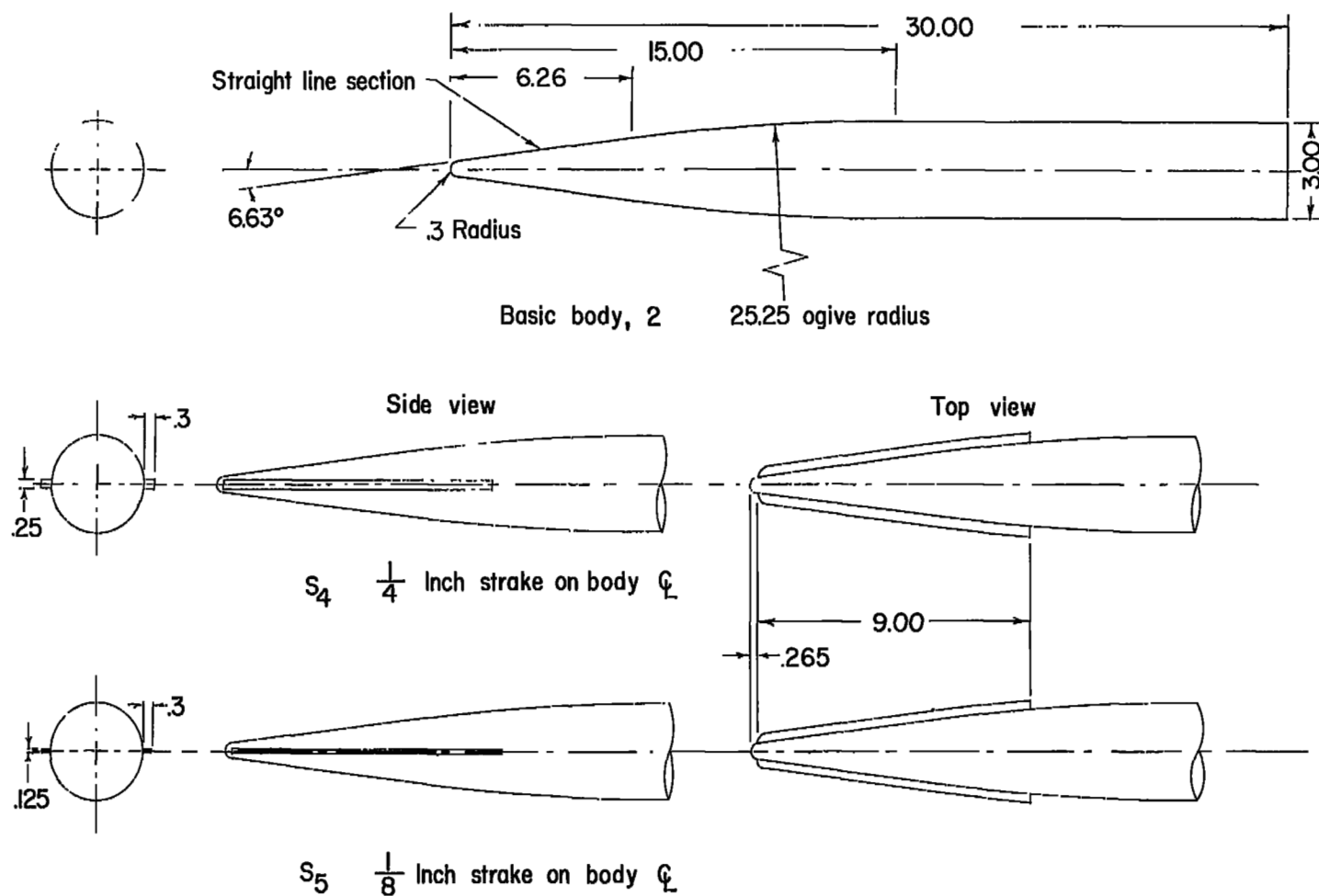
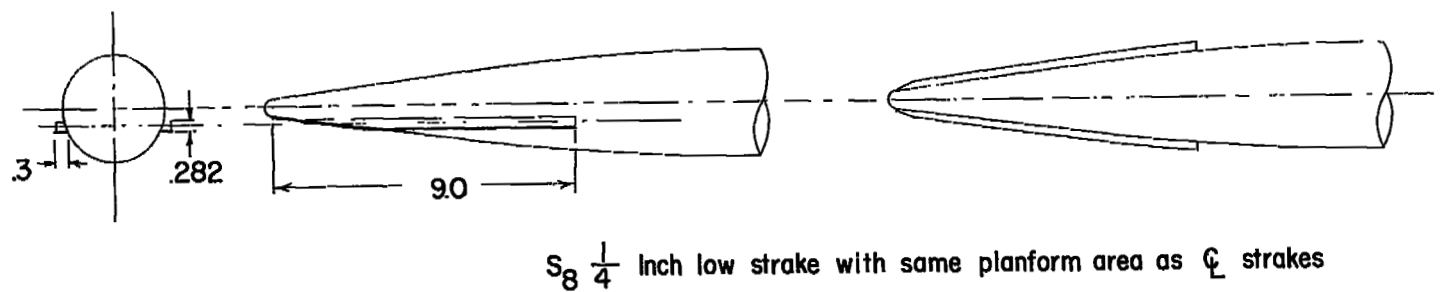
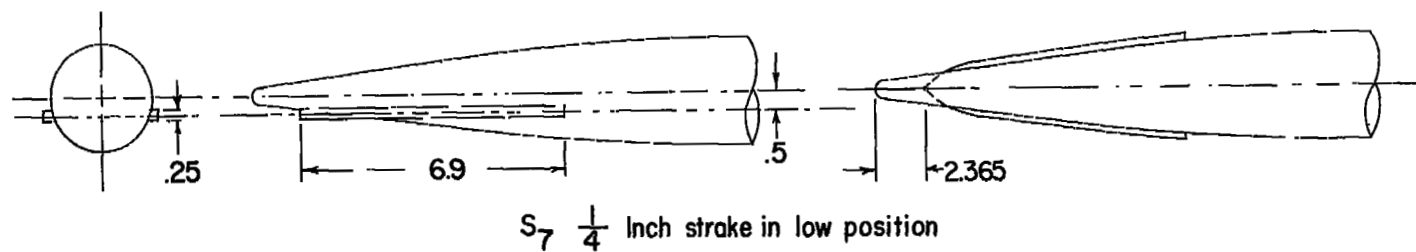
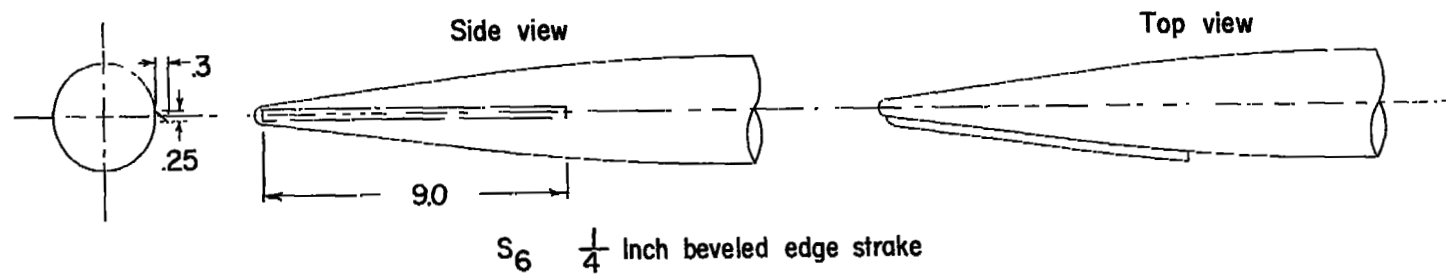


Figure 3.- Strake details for body 1.



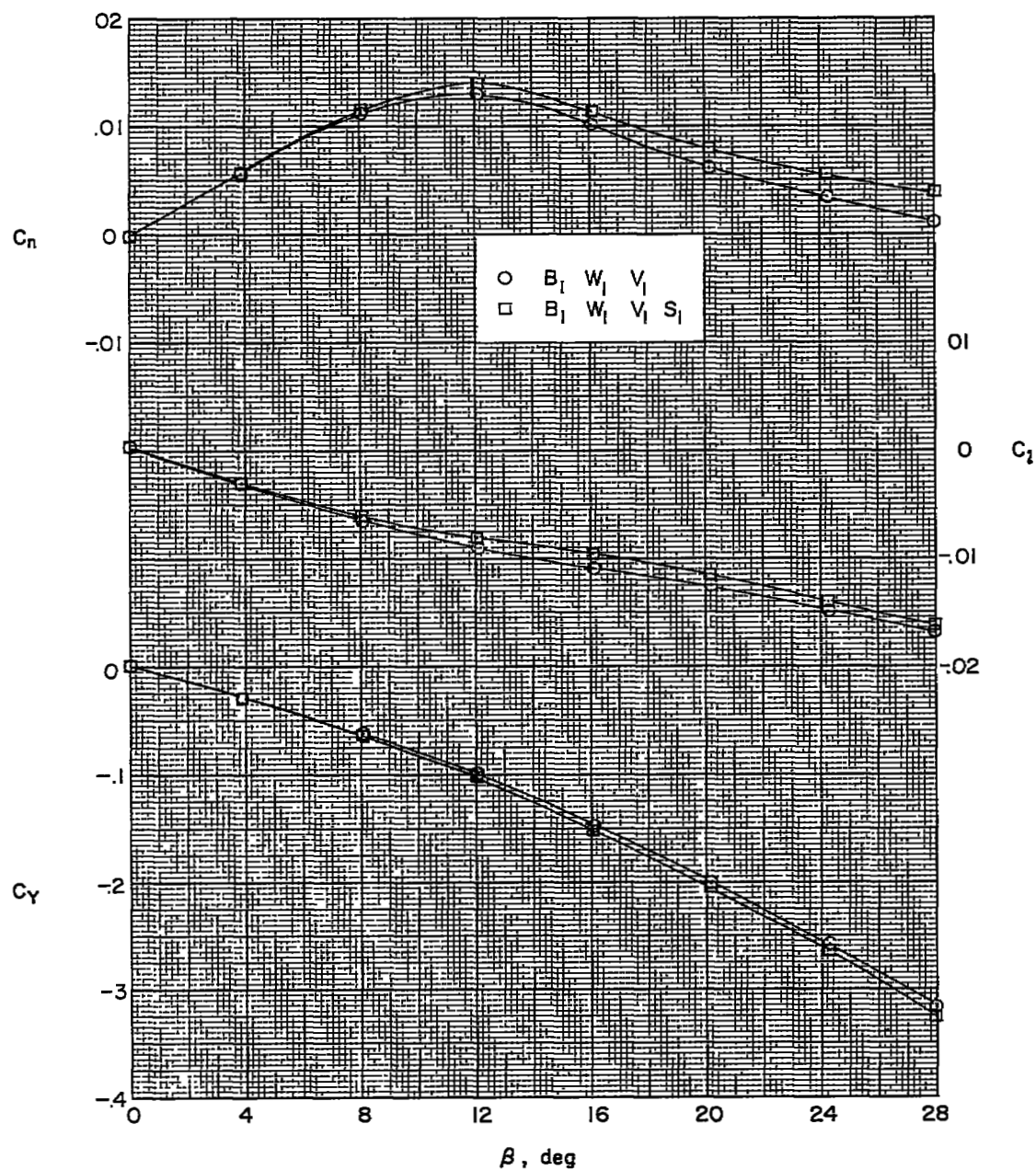
(a) Strakes, S<sub>4</sub> and S<sub>5</sub>.

Figure 4.- Strake details for body 2.



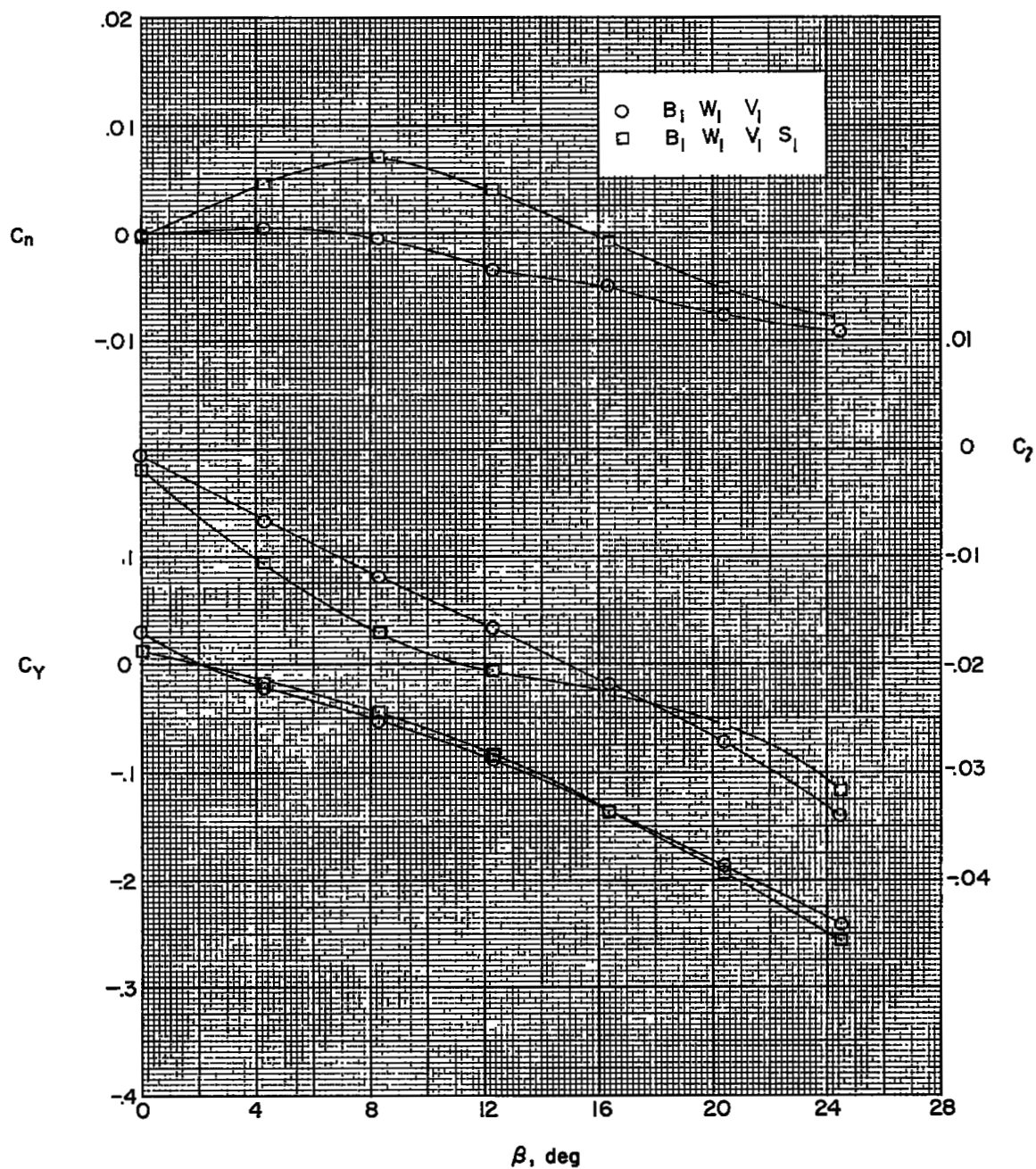
(b) Strakes,  $S_6$ ,  $S_7$ , and  $S_8$ .

Figure 4.- Concluded.



(a)  $\alpha = 0^\circ$ .

Figure 5.- Effect of strakes on lateral characteristics of configuration with body-mounted vertical tail.



(b)  $\alpha = 12.1^\circ$ .

Figure 5.- Concluded.

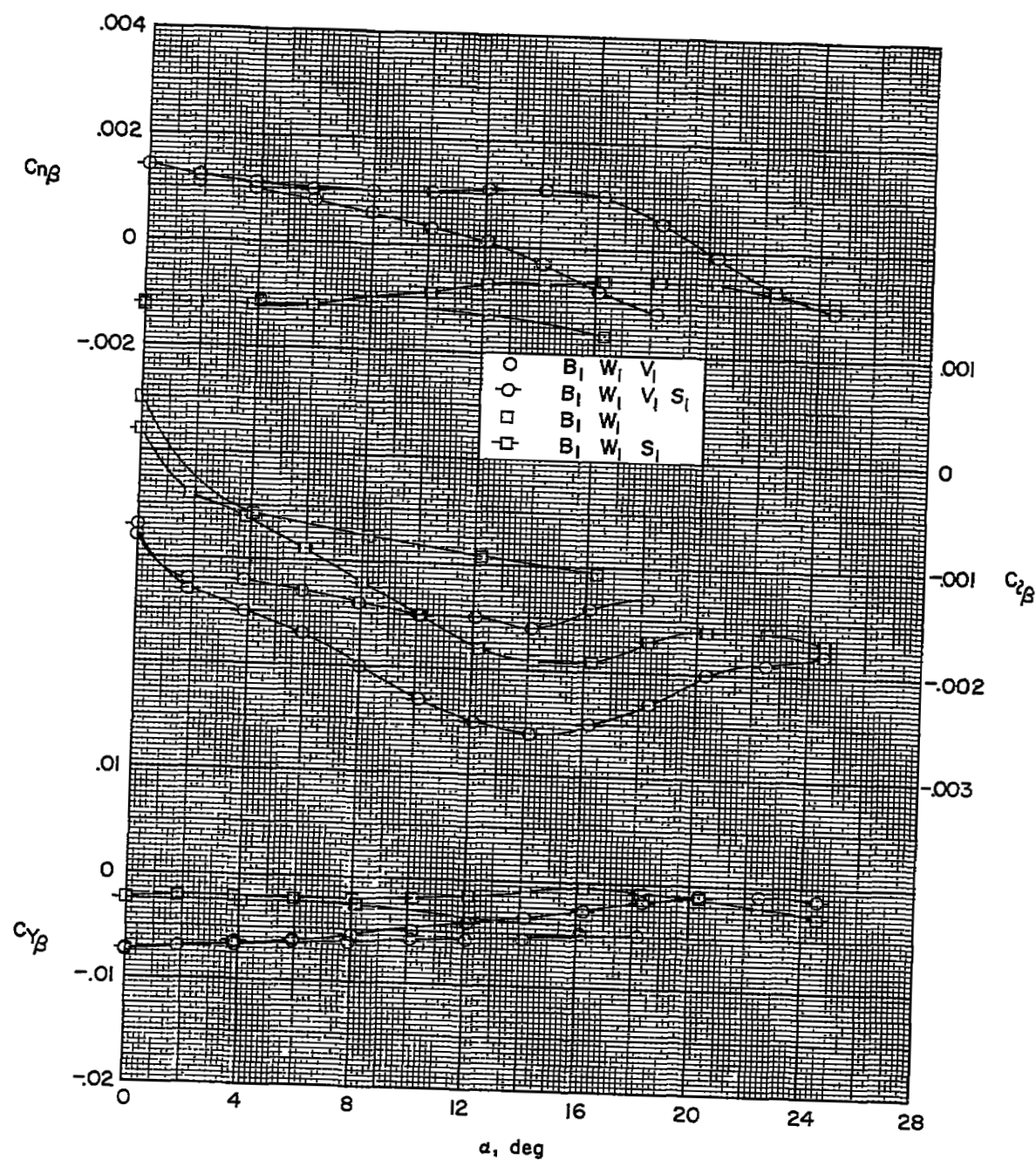


Figure 6.- Sideslip derivatives of configuration with body-mounted vertical tail.



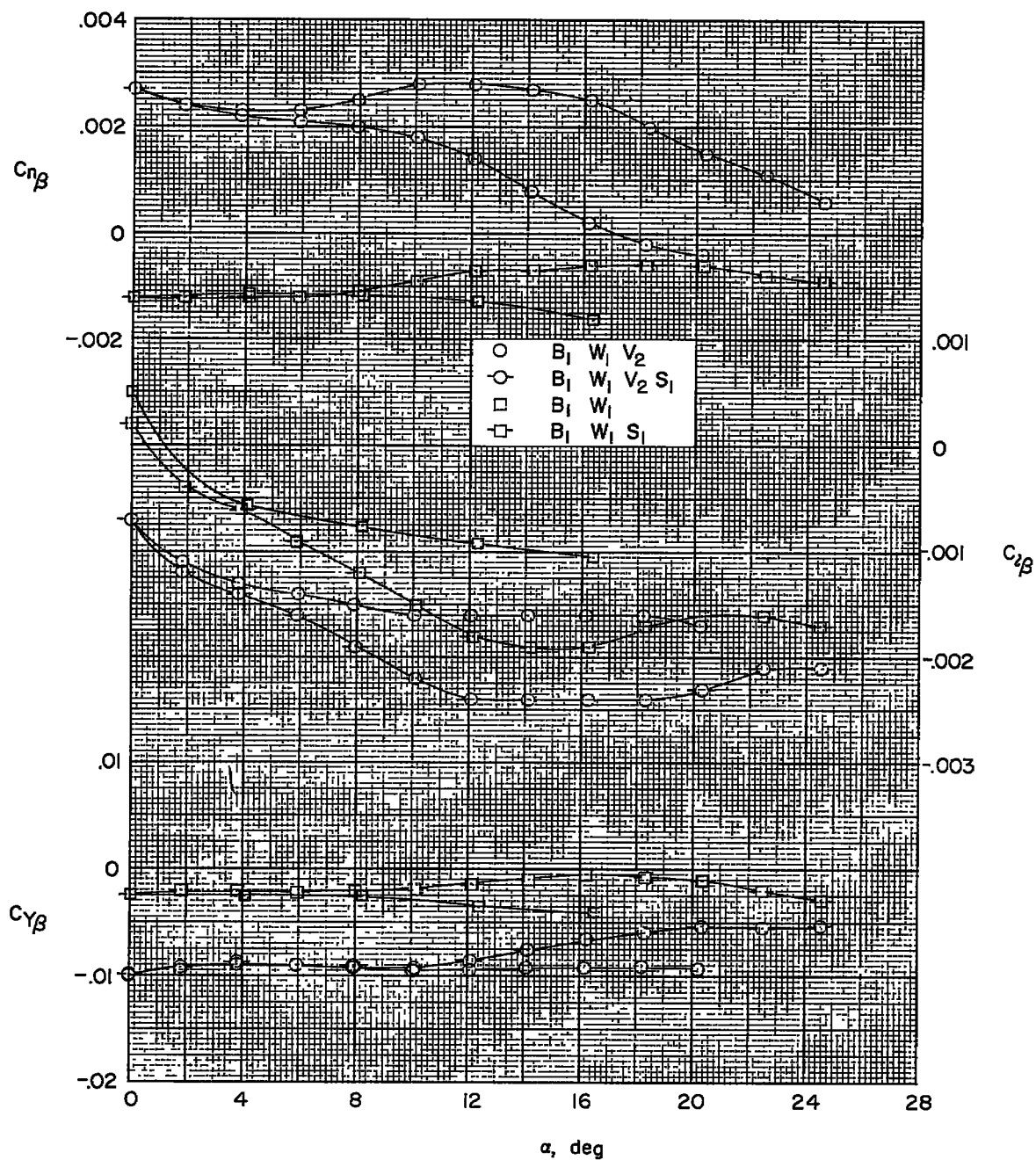


Figure 7.- Sideslip derivatives of configuration with wing-mounted vertical tails.

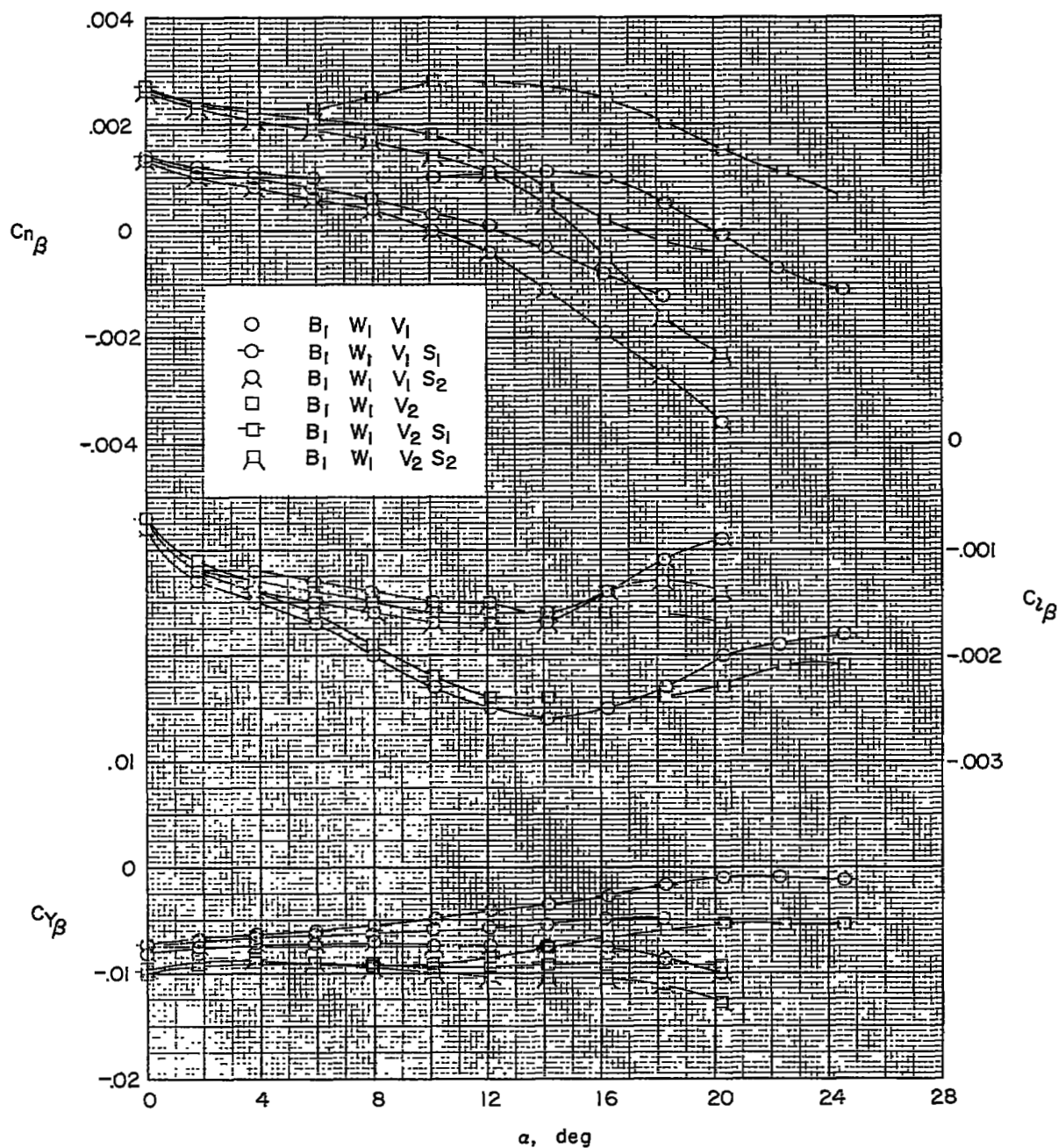


Figure 8.- Effect of strake position on lateral characteristics of both body-mounted and wing-mounted vertical-tail configurations.

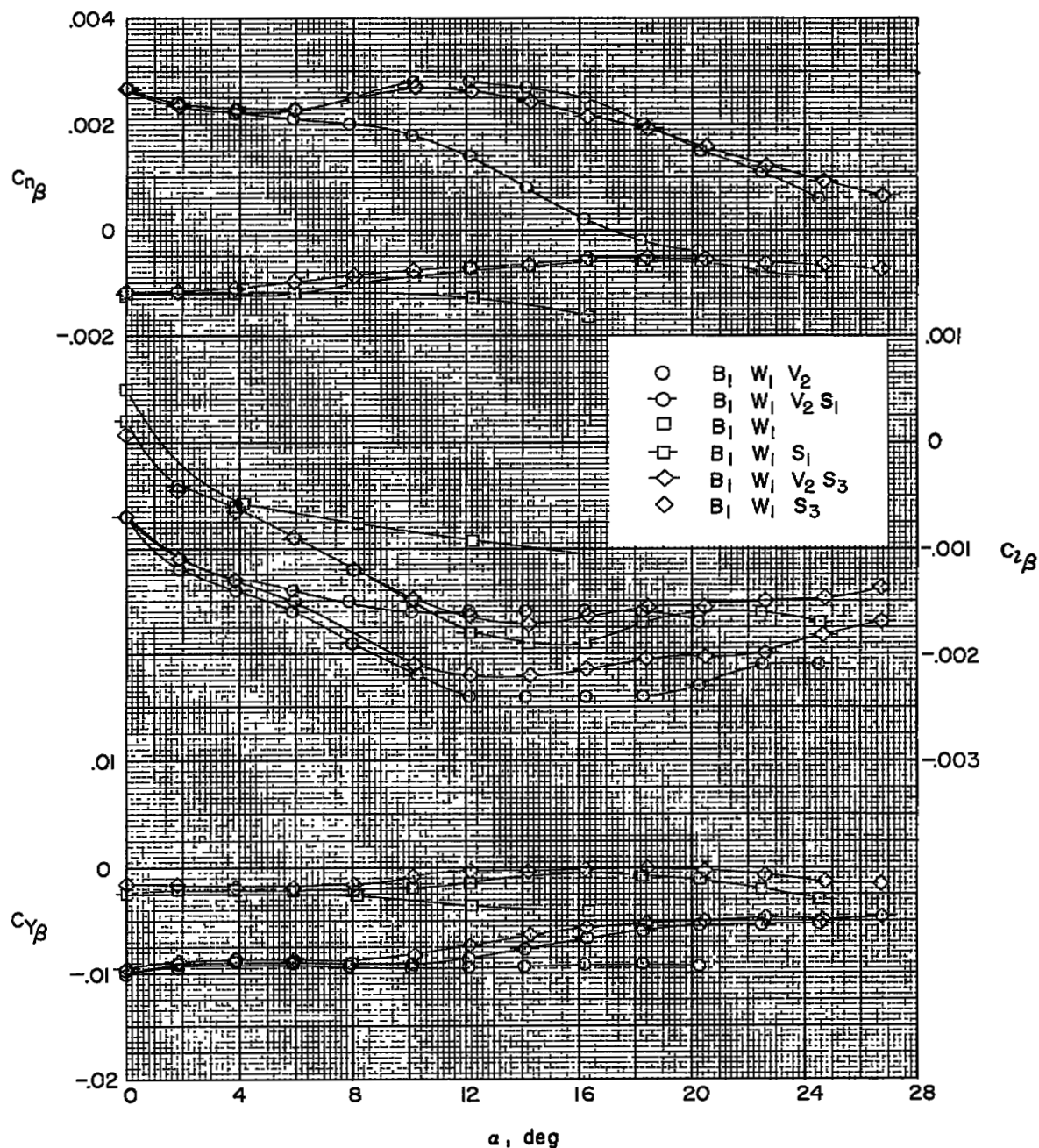


Figure 9.- Effect of strake length on lateral characteristics of wing-mounted vertical-tail configuration.

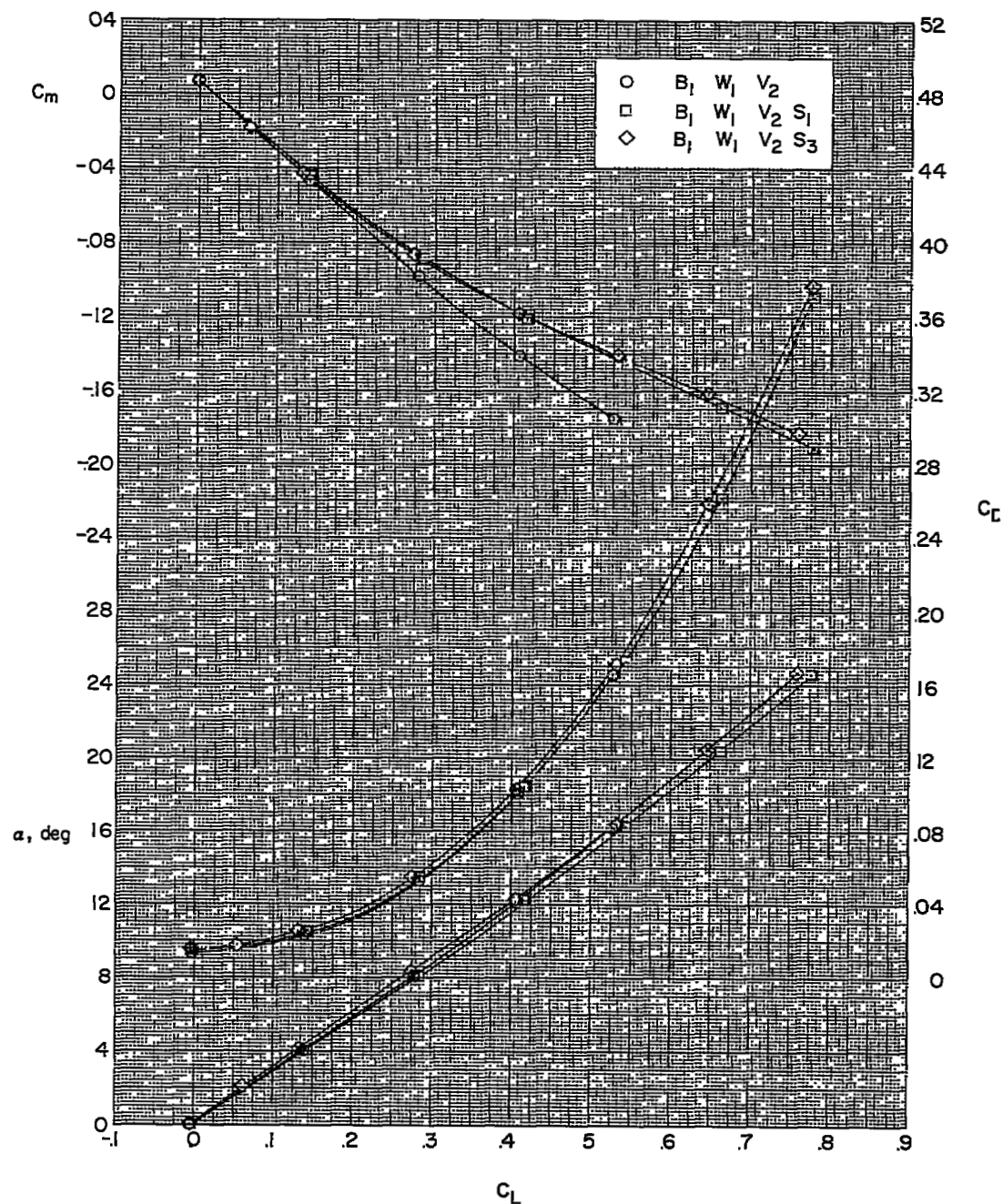


Figure 10.- Effect of strakes and of strake length on longitudinal characteristics of wing-mounted vertical-tail configuration.

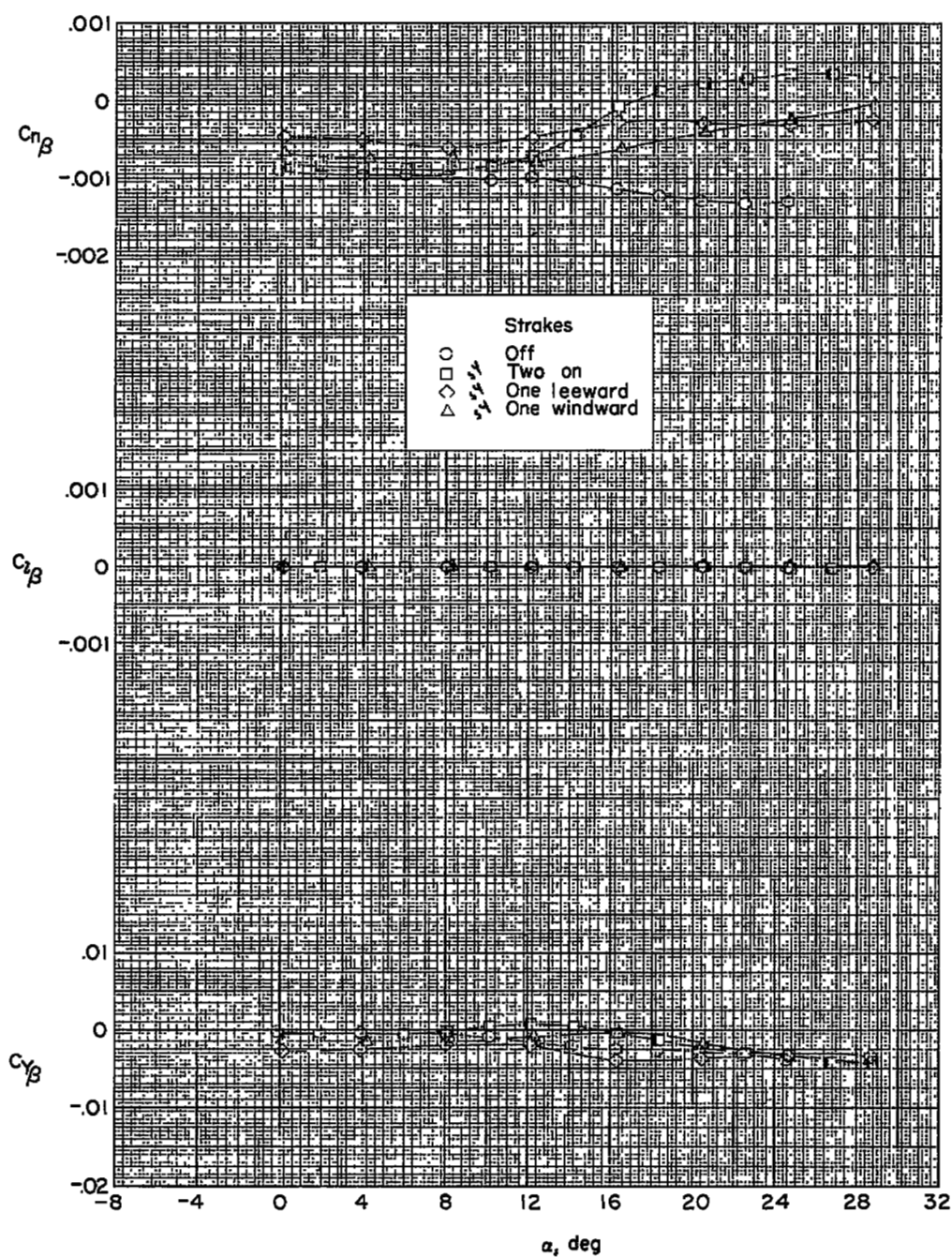


Figure 11.- Effect on lateral characteristics of the presence of 1/4-inch-thick strakes on the B<sub>2</sub> configuration.



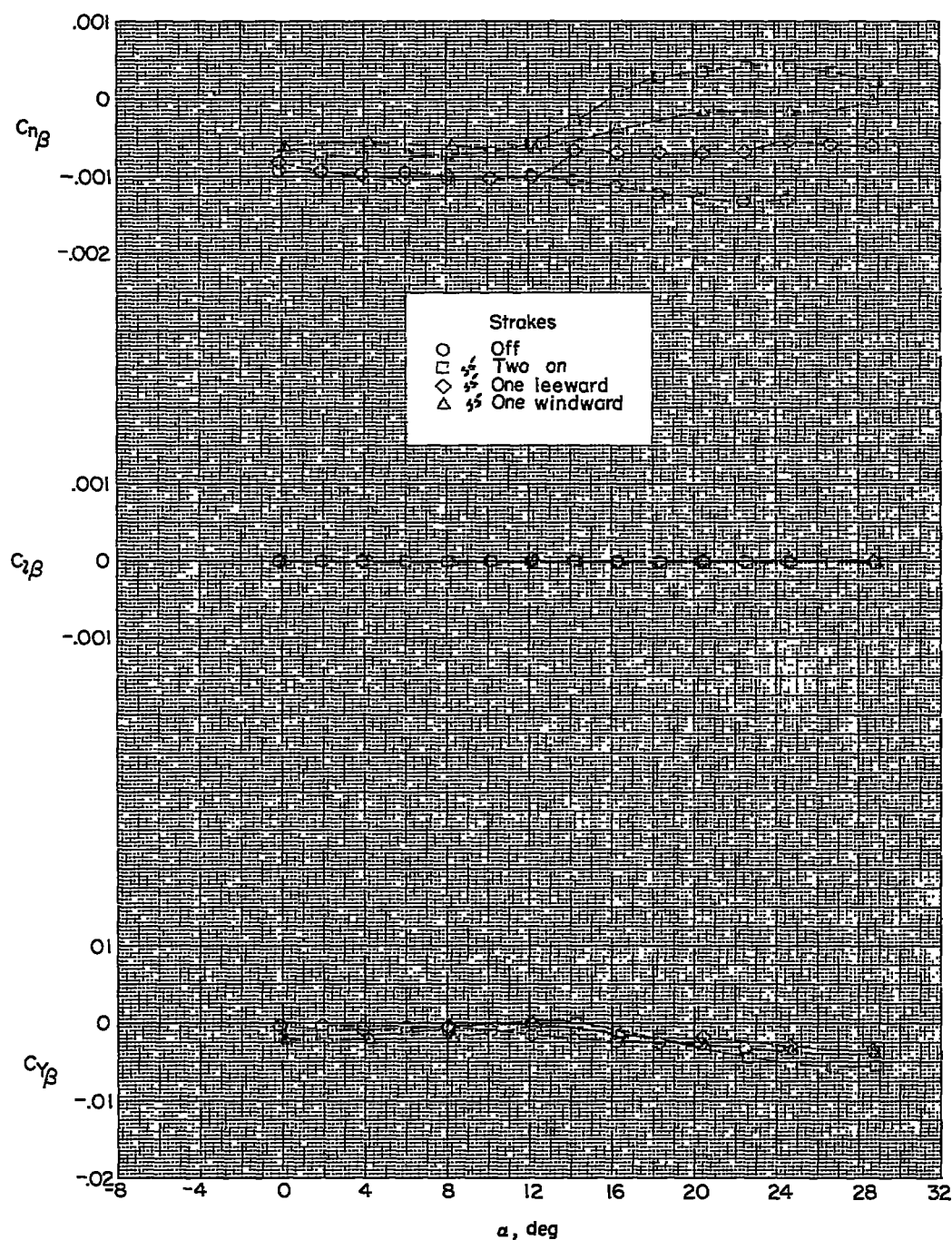


Figure 12.- Effect on lateral characteristics of the presence of 1/8-inch-thick strakes on the B<sub>2</sub> configuration.

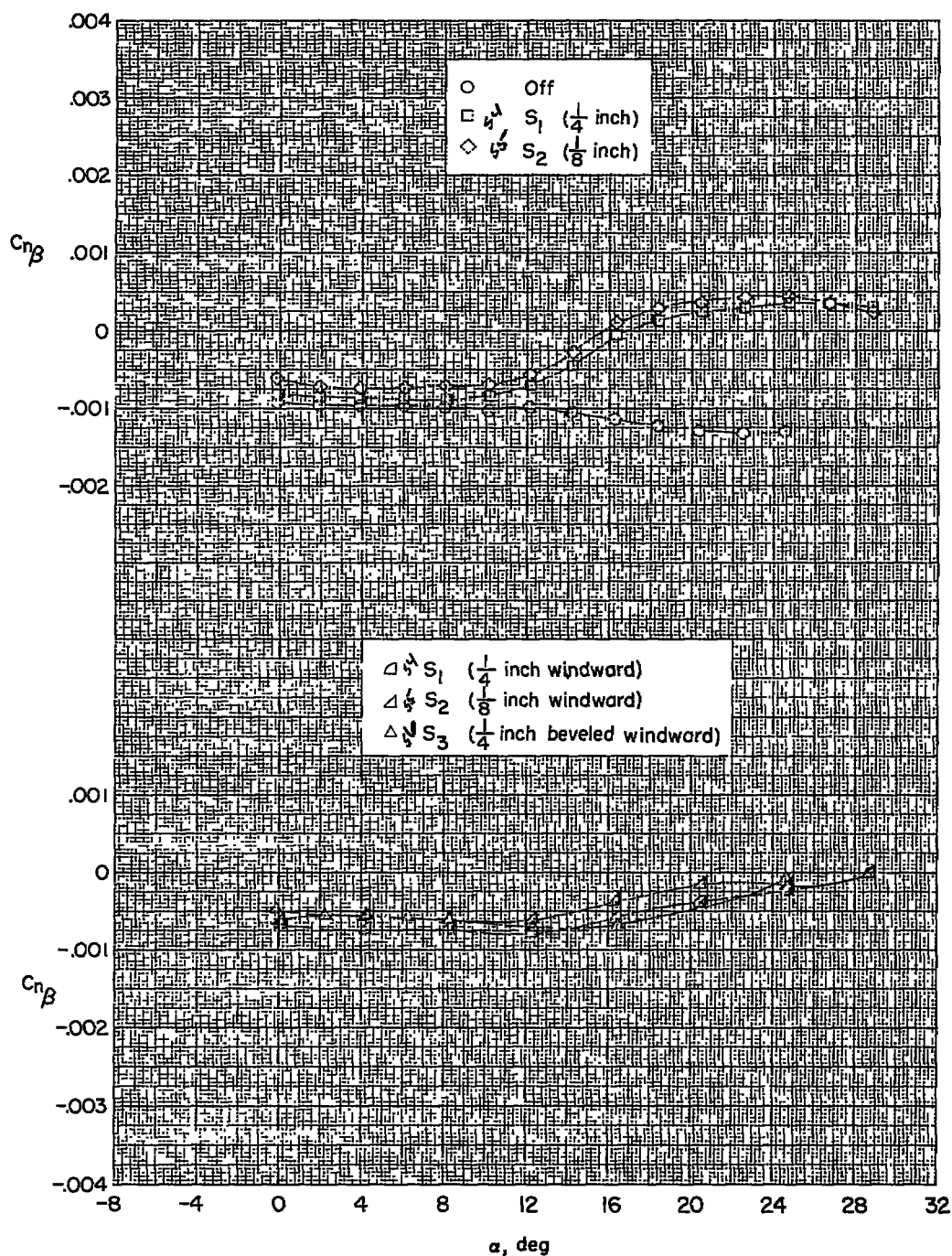


Figure 13.- Effect of strike thickness on lateral characteristics of the  $B_2$  configuration.

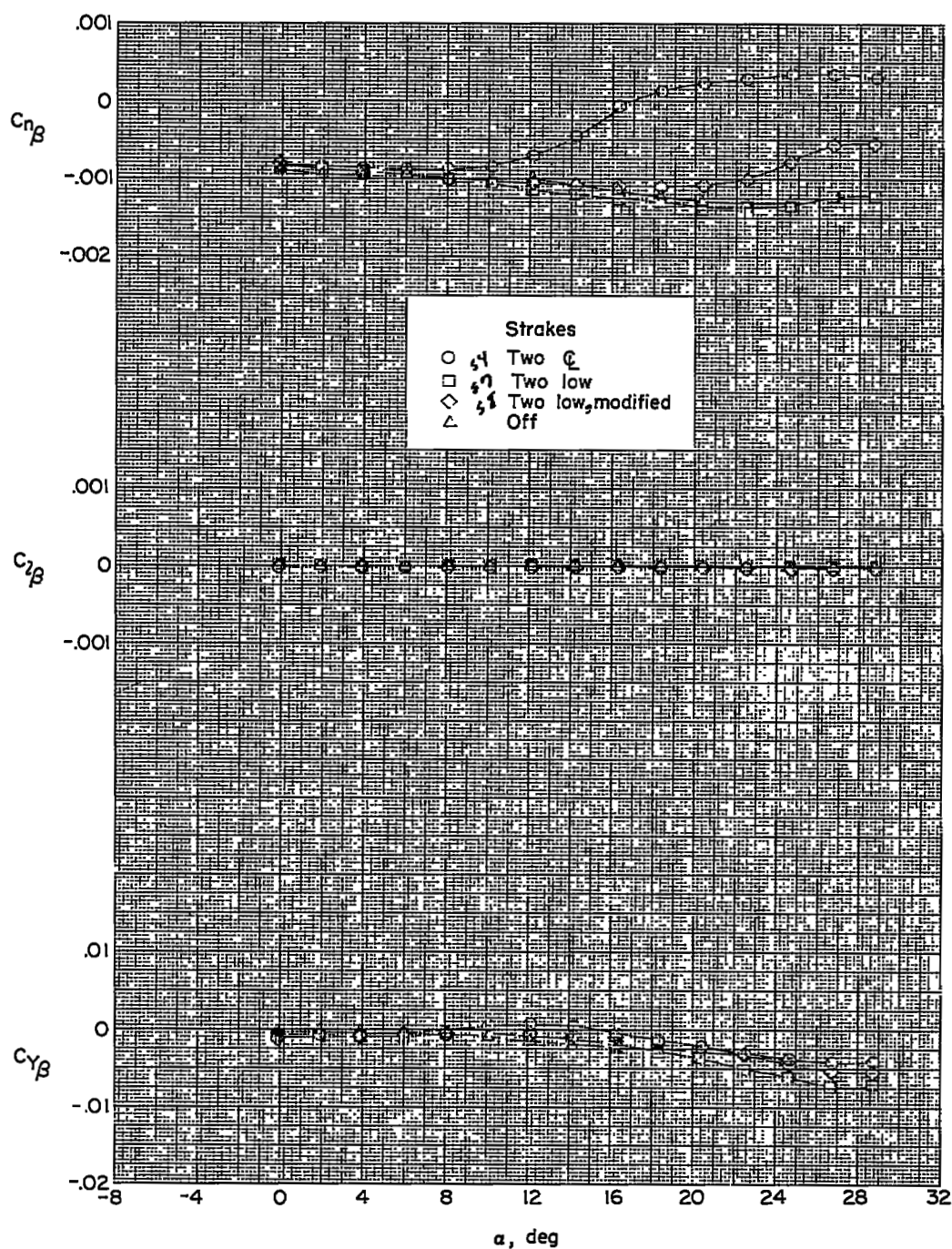


Figure 14.- Effect of strake vertical location on lateral characteristics of the  $B_2$  configuration.



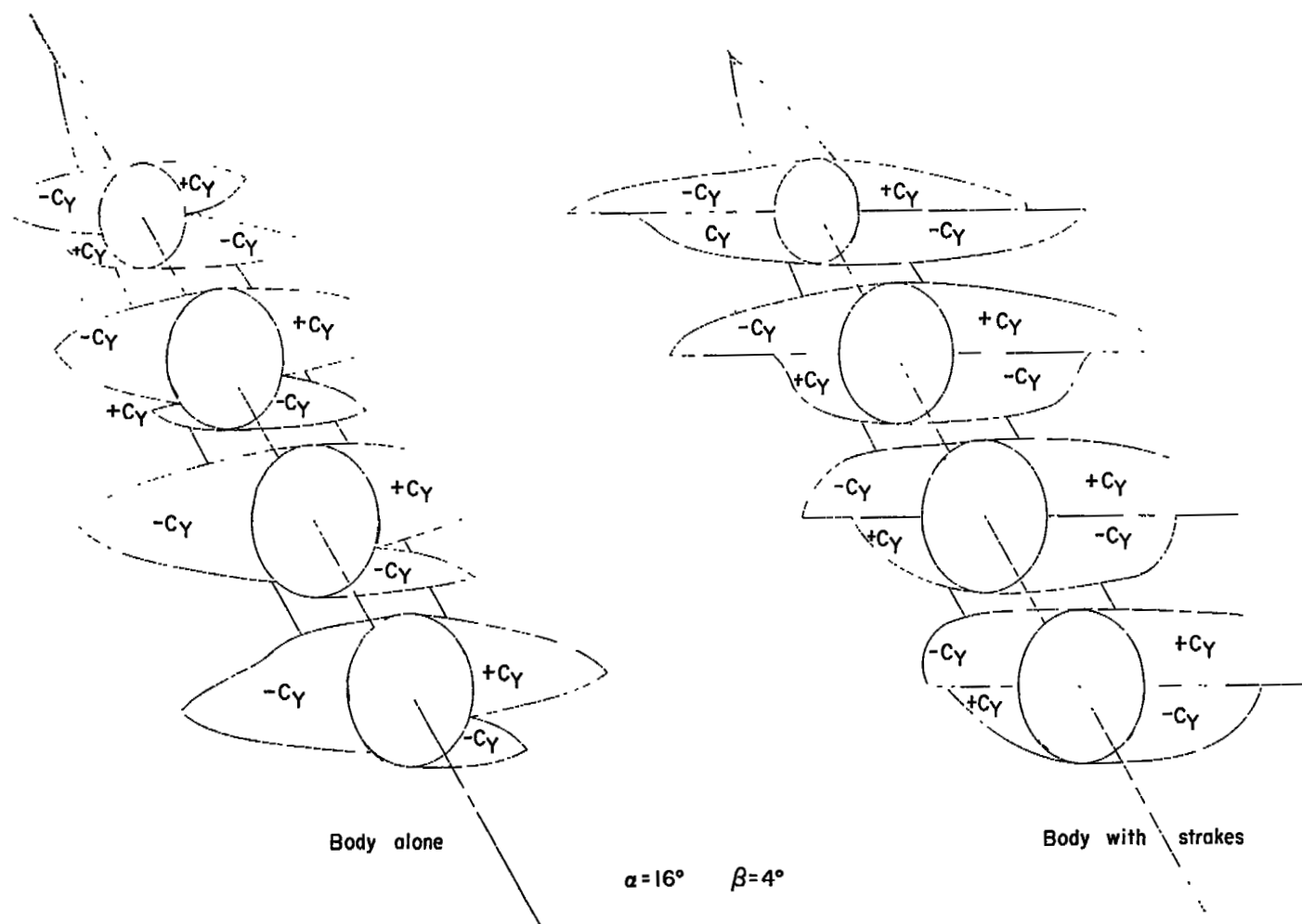


Figure 15.- Effect of strakes on the side-force component of radial pressure distributions for the forebody of the wing-body configuration.